



OPEN

# Long-range magnetic interaction and frustration in double perovskites $\text{Sr}_2\text{NiIrO}_6$ and $\text{Sr}_2\text{ZnIrO}_6$

SUBJECT AREAS:  
ELECTRONIC PROPERTIES  
AND MATERIALSMAGNETIC PROPERTIES AND  
MATERIALSXuedong Ou<sup>1</sup>, Zhengwei Li<sup>1</sup>, Fengren Fan<sup>1</sup>, Hongbo Wang<sup>1</sup> & Hua Wu<sup>2</sup>Received  
18 September 2014Accepted  
1 December 2014Published  
18 December 2014Correspondence and  
requests for materials  
should be addressed to  
H.W. (wuh@fudan.  
edu.cn)<sup>1</sup>Laboratory for Computational Physical Sciences (MOE), State Key Laboratory of Surface Physics, and Department of Physics, Fudan University, Shanghai 200433, China, <sup>2</sup>Collaborative Innovation Center of Advanced Microstructures, Nanjing 210093, China.

One often counts the nearest neighbouring (NN) exchange interactions for understanding of a magnetic insulator. Here we present first-principles calculations for the newly synthesized double perovskites  $\text{Sr}_2\text{NiIrO}_6$  and  $\text{Sr}_2\text{ZnIrO}_6$ , and we find that the 2NN Ir-Ir antiferromagnetic coupling is even stronger than the 1NN Ni-Ir ferromagnetic one. Thus, the leading antiferromagnetic interactions in the fcc Ir sublattice give rise to a magnetic frustration.  $\text{Sr}_2\text{NiIrO}_6$  and  $\text{Sr}_2\text{ZnIrO}_6$  hence appear very similarly as a distorted low-temperature antiferromagnet (probably, of type III). This work highlights the long-range magnetic interactions of the delocalized 5d electrons, and it also addresses why the spin-orbit coupling is ineffective here.

In the insulating transition-metal (TM) oxides, superexchange (SE) coupling of neighbouring magnetic ions via intermediate oxygen, according to the Goodenough-Kanamori-Anderson rules<sup>1</sup>, commonly plays a leading role in their magnetic order. One simple but useful rule is that for a linear M-O-M' exchange path, the SE would be antiferromagnetic (AF) [ferromagnetic (FM)] when the active orbitals of M and M' are same [different]. Fig. 1 (a) shows two  $d^1$  ions each having two orthogonal A-B levels and the same A-level occupation. Taking into account an effective hopping  $t$  between two ions associated with the charge fluctuation ( $d^1 + d^1 \rightarrow d^0 + d^2$ ) where the electron correlation Hubbard  $U$  is involved, an energy gain of an AF order (relative to a FM one) is proportional to  $t^2/U$  in a strong correlation limit ( $U \gg t$ ). Fig. 1 (b) shows two different  $d^1$  level occupations, and a FM stability against AF is proportional to  $t^2 J_H/U^2$  where  $J_H$  is a Hund exchange. This is the reason why a FM Mott insulator is often associated with orbital physics (e.g., an orbital ordering) and its  $T_C$  is much lower (due to the factor  $J_H/U \sim 1/5$ ) than the  $T_N$  of many AF Mott insulators.

In practice, it is often sufficient to consider the SE between the nearest neighbouring (NN) magnetic ions only. This approach applies with much success to numerous insulating 3d TM oxides, where the 3d electrons are quite localized due to the strong correlation effect. In recent years, 5d TM oxides have received considerable attention due to their significant spin-orbit coupling (SOC) effect and possibly exotic properties<sup>2–10</sup>. The hybrid 3d–5d TM oxides are also of current great interest for exploration of novel magnetic and electronic properties in this material system, in which new SOC effects add to the common charge-spin-orbital physics appearing in the 3d TM oxides. Among them, the double perovskites  $\text{A}_2\text{BB}'\text{O}_6$  (A = alkaline earth metal, B = 3d TM, and B' = 5d TM) are an important material platform<sup>11–22</sup>:  $\text{Sr}_2\text{FeReO}_6$  is an above room temperature (RT) ferrimagnetic half metal<sup>11</sup>, and  $\text{Sr}_2\text{CrOsO}_4$  is a ferrimagnetic insulator with a seemingly highest  $T_C$  in the perovskite oxides<sup>13,14</sup>, etc. As 5d electrons are moderately or weakly correlated and their orbitals are much delocalized, their magnetic coupling could well be a long-range interaction.

In this work, we study the electronic structure and magnetism of the newly synthesized double perovskite  $\text{Sr}_2\text{NiIrO}_6$ <sup>17</sup>, using density functional calculations. This material crystallizes in the monoclinic space group P21/n at RT (see Fig. 2) and undergoes two structural phase transitions ( $\text{P21/n} \rightarrow \text{I4/m} \rightarrow \text{Fm-3m}$ ) upon heating. Magnetic susceptibility measurements<sup>17</sup> suggest the establishment of AF interactions at  $T_N = 58$  K. This oxide has the  $\text{Ni}^{2+}$  ( $t_{2g}^6 e_g^2$ )- $\text{Ir}^{6+}$  ( $t_{2g}^3$ ) charge state as seen below. Taking into account a charge fluctuation into the common  $\text{Ni}^{3+}$ - $\text{Ir}^{5+}$  state (a reverse  $\text{Ni}^{3+}$ - $\text{Ir}^{7+}$  is quite unusual), both the Ni up-spin  $e_g$  and down-spin  $t_{2g}$  electron hopping (the Ni up-spin  $t_{2g}$  levels lie lowest due to the crystal field splitting and Hund exchange) would give a FM SE between the  $\text{Ni}^{2+}$  and  $\text{Ir}^{6+}$  ions, see Figs. 1(c) and 1(d). As the  $e_g$  and  $t_{2g}$  levels are orthogonal, the  $e_g$  ( $t_{2g}$ ) electron hopping follows the simple SE mechanism plotted in Fig. 1(b) [Fig. 1(a)]. Apparently, this expected FM order contradicts the observed AF in  $\text{Sr}_2\text{NiIrO}_6$ , and thus consideration of only NN  $\text{Ni}^{2+}$ - $\text{Ir}^{6+}$  coupling would be a

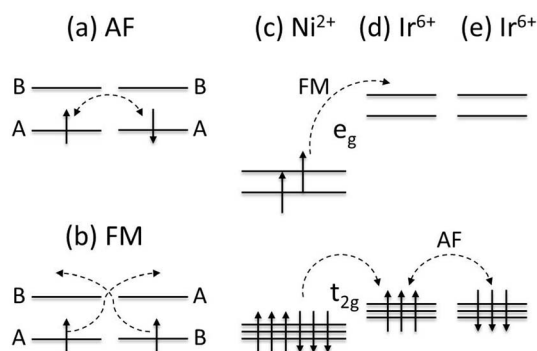


**Figure 1** | (a) AF and (b) FM SE between two two-level d<sup>1</sup> ions. (c) and (d): Sr<sub>2</sub>NiIrO<sub>6</sub> would be FM, according to the SE between the NN Ni<sup>2+</sup> and Ir<sup>6+</sup> ions. (d) and (e): AF SE in the fcc Ir<sup>6+</sup> sublattice.

mistake here. Then, a possibly long-ranged Ir-Ir coupling within the fcc sublattice should be invoked, which would be AF due to the half-filled t<sub>2g</sub> shells [Figs. 1(d) and 1(e)]. As we calculate below, there is indeed a long-range AF interaction in the fcc Ir<sup>6+</sup> sublattice, and the second NN Ir-Ir AF coupling energy is even bigger than the first NN Ni-Ir FM one, thus giving rise to a magnetic frustration<sup>23–26</sup>. As a result, Sr<sub>2</sub>NiIrO<sub>6</sub> behaves as a distorted low-temperature antiferromagnet<sup>17</sup> (probably, of type III)<sup>24–26</sup>. Naturally, the frustrated AF couplings in the fcc Ir<sup>6+</sup> sublattice explain a very similar magnetic property in the isostructural Sr<sub>2</sub>ZnIrO<sub>6</sub><sup>17</sup>. Note that one could take care of long-range magnetic interaction of the delocalized 5d electrons.

## Results

We first study the electronic structure of Sr<sub>2</sub>NiIrO<sub>6</sub> and the Ni-Ir charge state. Fig. 3 shows the orbitally resolved density of states (DOS) calculated by LSDA for the FM state. The delocalized Ir 5d electrons have a strong covalency with the ligand oxygens, giving rise to a large bonding-antibonding splitting. The pdσ splitting of the Ir e<sub>g</sub> electrons is up to 9 eV, and the pdπ splitting of the Ir t<sub>2g</sub> electrons is about 6 eV. The Ir 5d electrons have a t<sub>2g</sub>-e<sub>g</sub> crystal-field splitting of more than 3 eV. Besides the occupied bonding states (around -6 eV) ascribed to the lower-lying O 2p bands, only the up-spin Ir t<sub>2g</sub> state is occupied, giving a formal Ir<sup>6+</sup> charge state with a t<sup>3</sup><sub>2g</sub> (S = 3/2) configuration. In contrast, the Ni 3d electrons are confined and have a smaller pdσ (pdπ) bonding-antibonding splitting of 4 eV

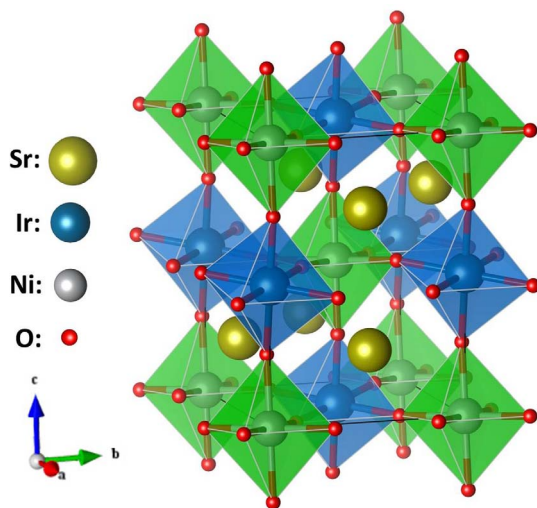


**Figure 2** | Double perovskite structure of Sr<sub>2</sub>NiIrO<sub>6</sub>. The Ni and Ir ions form their respective fcc sublattices.

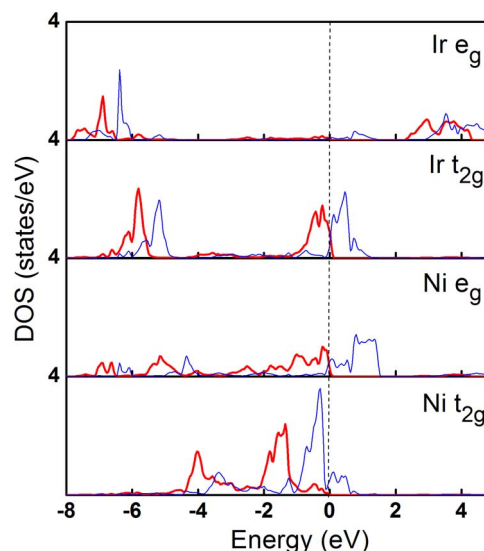


**Figure 3** | Ir 5d and Ni 3d DOS of Sr<sub>2</sub>NiIrO<sub>6</sub> calculated by LSDA for the FM state. The solid red (thin blue) curves stand for the up (down) spin channel. Fermi level is set at zero energy. Sr<sub>2</sub>NiIrO<sub>6</sub> has the Ni<sup>2+</sup> (t<sup>6</sup><sub>2g</sub>e<sup>2</sup><sub>g</sub>)-Ir<sup>6+</sup> (t<sup>3</sup><sub>2g</sub>) charge state.

(2 eV) and the t<sub>2g</sub>-e<sub>g</sub> crystal-field splitting of 1–1.5 eV. Only the down-spin Ni e<sub>g</sub> antibonding state is unoccupied, giving a formal Ni<sup>2+</sup> charge state with the t<sup>6</sup><sub>2g</sub>e<sup>2</sup><sub>g</sub> (S = 1) configuration. Therefore, Sr<sub>2</sub>NiIrO<sub>6</sub> has the Ni<sup>2+</sup>-Ir<sup>6+</sup> charge state. Its closed subshells and a finite electron correlation would certainly make Sr<sub>2</sub>NiIrO<sub>6</sub> insulating. However, in the present LSDA calculation, the bandwidth of the Ir t<sub>2g</sub> electrons is slightly larger than the exchange splitting, making the Ir t<sub>2g</sub> bands of two spin directions somewhat overlapping at the Fermi level. As seen below, this metallic solution will turn into a Mott insulating one upon inclusion of the electron correlation.

We now include the static electron correlation by carrying out LSDA + U calculations. The insulating band structure is shown in Fig. 4. It has a small band gap of 0.3 eV within the Ir t<sub>2g</sub> bands due to the moderate electron correlation of the delocalized Ir 5d electrons. The Ni 3d bands have a gap of more than 2 eV due to the strong correlation. The electron correlation enhances electron localization and reduces band hybridization and further stabilizes the Ni<sup>2+</sup>-Ir<sup>6+</sup> charge state. The Ni<sup>2+</sup> (S = 1) ion has a spin moment of 1.76 μ<sub>B</sub> (see Table 1), being close to its formal value of 2 μ<sub>B</sub>. The Ir<sup>6+</sup> (S = 3/2) ion has a smaller moment of 1.46 μ<sub>B</sub> reduced by the strong covalency with the oxygen ligands. Note that we also test the Ni<sup>3+</sup>-Ir<sup>5+</sup> state, using constrained LSDA + U calculations. We initialize the corresponding occupation number matrix and the orbital polarized potential, and consider a possible J = 0 singlet state of the Ir<sup>5+</sup> ion due to its strong SOC. After a full electronic relaxation, however, the self-consistent LSDA + U + SOC calculations converge also to the present Ni<sup>2+</sup>-Ir<sup>6+</sup> state.

As both the Ni<sup>2+</sup> and Ir<sup>6+</sup> ions are magnetic and form their respective fcc sublattices, their magnetic interactions are of concern. Here we study different magnetic structures using LSDA + U calculations. The G-AF state of Sr<sub>2</sub>NiIrO<sub>6</sub> (FM Ni<sup>2+</sup> and Ir<sup>6+</sup> sublattices being AF coupled) turns out to be less stable than the FM state by 89 meV/fu, see Table 1. As the FM and G-AF states differ in the exchange energy only by the 1NN Ni-Ir couplings, which are ±6J<sub>Ni-Ir</sub> per formula unit. Then the average exchange energy parameter of the 1NN Ni-Ir pairs can be estimated to be J<sub>Ni-Ir</sub> = -89/12 ≈ -7.4 meV. This FM Ni-Ir coupling is readily understood by a SE mechanism, see Fig. 1 and the Introduction. However, the observed AF interaction<sup>17</sup> at T<sub>N</sub> = 58 K questions this description. Therefore, we are motivated to study the long-range magnetic interactions,

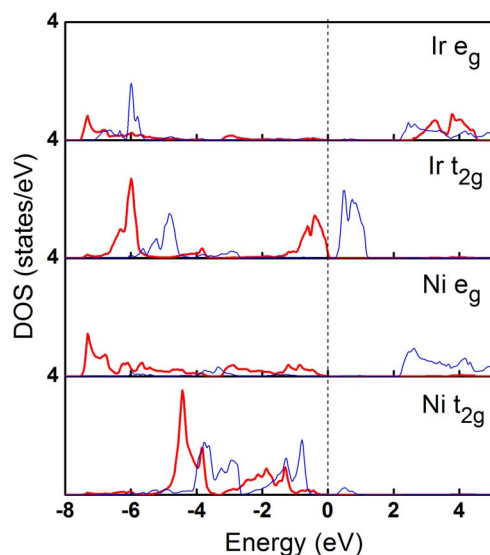


**Figure 4** | Insulating band structure of  $\text{Sr}_2\text{NiIrO}_6$  in the  $\text{Ni}^{2+}$  ( $t_{2g}^6 e_g^2$ )- $\text{Ir}^{6+}$  ( $t_{2g}^6$ ) charge state calculated by LSDA + U for the FM state. Other magnetic states have a very similar band structure.

particularly those associated with the delocalized Ir 5d electrons. To do so, we use two artificial systems with either  $\text{Ir}^{6+}$  or  $\text{Ni}^{2+}$  magnetic sublattice only,  $\text{Sr}_2\text{ZnIrO}_6$  [i.e.,  $\text{Sr}_2\text{Zn}(\text{Ni})\text{IrO}_6$  in Table 1] and  $\text{La}_2\text{NiSiO}_6$  both in the  $\text{Sr}_2\text{NiIrO}_6$  structure, to calculate the 2NN  $\text{Ir}^{6+}$ - $\text{Ir}^{6+}$  and  $\text{Ni}^{2+}$ - $\text{Ni}^{2+}$  exchange parameters ( $J'_{\text{Ir-Ir}}$  and  $J'_{\text{Ni-Ni}}$  with a reference to the 1NN  $J_{\text{Ni-Ir}}$ ). This approach avoids choices of complicate magnetic structures in bigger supercells, and allows to estimate the two parameters separately. For  $\text{Sr}_2\text{Zn}(\text{Ni})\text{IrO}_6$ , the layered AF state (FM ab planes being AF alternate along the c axis, see also Fig. 2) is more stable than the FM state by 84 meV/fu, see Table 1. The layered AF and FM states differ in the exchange energy only by the 2NN Ir-Ir couplings (with a reference to the 1NN Ni-Ir ones), i.e.,  $-2J'_{\text{Ir-Ir}}$  vs  $6J'_{\text{Ir-Ir}}$ . Then the energy difference gives AF  $J'_{\text{Ir-Ir}} = 84/8 = 10.5$  meV. The corresponding energy difference of 19 meV/fu for  $\text{La}_2\text{NiSiO}_6$  gives AF  $J'_{\text{Ni-Ni}} = 19/8 \approx 2.4$  meV, see Table 1.

As the magnetic  $\text{Ir}^{6+}$  and  $\text{Ni}^{2+}$  ions have closed subshells, the SE interactions naturally explain the AF  $J'_{\text{Ir-Ir}}$  and  $J'_{\text{Ni-Ni}}$ . Note that the  $\text{Ni}^{2+}$  3d electrons are confined but the  $\text{Ir}^{6+}$  5d electrons are delocalized, it is therefore not surprising that  $J'_{\text{Ir-Ir}}$  is about four times as big as  $J'_{\text{Ni-Ni}}$ . However, it is a bit surprising that the 2NN AF  $J'_{\text{Ir-Ir}}$  is even bigger than the 1NN FM  $J_{\text{Ni-Ir}}$ , thus giving rise to a magnetic frustration in  $\text{Sr}_2\text{NiIrO}_6$ . This vital role of the strong 2NN AF Ir-Ir

coupling is also manifested in the real double perovskite  $\text{Sr}_2\text{ZnIrO}_6$ , see below.

$\text{Sr}_2\text{ZnIrO}_6$  has a very similar crystal structure and magnetic property to  $\text{Sr}_2\text{NiIrO}_6$ , and it has AF interactions at  $T_N = 46$  K<sup>17</sup>. We have also calculated different magnetic states of  $\text{Sr}_2\text{ZnIrO}_6$  and find the 2NN AF  $J'_{\text{Ir-Ir}} = 75/8 \approx 9.4$  meV (see Table 1), being close to  $J'_{\text{Ir-Ir}} = 10.5$  meV in  $\text{Sr}_2\text{NiIrO}_6$ . As the delocalized Ir 5d electrons produce a long-range magnetic interaction, we also estimate the 3NN AF  $J''_{\text{Ir-Ir}}$  (the exchange path along the linear Ir-O-Ni-O-Ir bonds with the Ir-Ir distance of 7.8 Å) by calculating the bilayered AF state of  $\text{Sr}_2\text{ZnIrO}_6$ . The bilayered AF state has FM ab planes but AF alternation every bilayer along the c axis, and it is more stable than the FM state by 42 meV/fu. The exchange energy per formula unit can be expressed as  $6J'_{\text{Ir-Ir}} + 3J''_{\text{Ir-Ir}}$  for the FM state and  $2J'_{\text{Ir-Ir}} + J''_{\text{Ir-Ir}}$  for the bilayered AF state. Therefore, the AF  $J''_{\text{Ir-Ir}}$  is estimated to be  $(42 - 4 \times 9.4)/2 = 2.2$  meV.

## Discussion

As seen from the above results, apparently the Ir-Ir magnetic interactions are long-ranged and have a non-negligible strength even at a distance of about 8 Å. It is the long-range AF interactions of the  $\text{Ir}^{6+}$  sublattice which make  $\text{Sr}_2\text{ZnIrO}_6$  magnetically frustrated. As both  $J'_{\text{Ir-Ir}} = 9.4$  meV and  $J''_{\text{Ir-Ir}} = 2.2$  meV (see Table 1) are AF, and  $J''_{\text{Ir-Ir}}/J'_{\text{Ir-Ir}} < 1/2$ ,  $\text{Sr}_2\text{ZnIrO}_6$  is most probably a type-III anti-ferromagnet<sup>24-26</sup>. Moreover, while the strongest 2NN AF  $J'_{\text{Ir-Ir}}$  overwhelms the 1NN FM  $J_{\text{Ni-Ir}}$  and also makes  $\text{Sr}_2\text{NiIrO}_6$  magnetically frustrated, the FM  $J_{\text{Ni-Ir}}$  could lift (or at least, partially) the frustration and select one state out of the degenerate manifold of fcc AF. In a word, the long-range magnetic interactions and frustration would make the cubic double perovskites  $\text{Sr}_2\text{NiIrO}_6$  and  $\text{Sr}_2\text{ZnIrO}_6$  distorted, and this would partially relieve the magnetic frustration and eventually stabilize them into a similar low-temperature anti-ferromagnet<sup>17</sup> which is worth a further experimental study.

Finally, we check if the SOC is important or not in the present materials. Normally, SOC is important in heavy 5d TMs, and particularly, iridates recently receive great interest<sup>2-10</sup>. Owing to a large crystal-field splitting, iridates are in a low-spin state with only the  $t_{2g}$  occupation (e.g., in a cubic crystal field). Then the SOC splits the  $t_{2g}$  triplet (with also 2-fold spin degeneracy) into the lower  $J = 3/2$  quartet and the higher  $J = 1/2$  doublet<sup>2,3</sup>. We have used this SOC basis set to project the  $\text{Ir}^{6+}$   $t_{2g}$  DOS of  $\text{Sr}_2\text{ZnIrO}_6$  calculated by LDA + SOC, but we find that the  $J = 3/2$  and the  $J = 1/2$  states are completely mixed, see Fig. 5(a). Therefore, the  $J = 3/2$  and the  $J = 1/2$  states are not at all eigen orbitals in  $\text{Sr}_2\text{ZnIrO}_6$  (and in  $\text{Sr}_2\text{NiIrO}_6$  with the same fcc  $\text{Ir}^{6+}$  sublattice). This is because the delocalized Ir 5d electrons form, with the intersite electron hoppings in the fcc sublattice (the high coordination of twelve), a 'broad' band with its bandwidth being more than 1 eV. Then the SOC effect is 'killed'.

**Table 1** | Relative total energies  $\Delta E$  (meV/fu) and spin moments  $M$  (in unit of  $\mu_B$ ) calculated by LSDA + U for different systems in different magnetic states. The Ir-Ir magnetic interactions are estimated for  $\text{Sr}_2\text{ZnIrO}_6$  either in  $\text{Sr}_2\text{NiIrO}_6$  structure (Zn substitution for Ni) or in its real structure<sup>17</sup>. The Ni-Ni exchange coupling is estimated using the artificial  $\text{La}_2\text{NiSiO}_6$  in  $\text{Sr}_2\text{NiIrO}_6$  structure. The derived exchange energy parameters (meV) for the 1NN Ni-Ir, 2NN Ir-Ir and Ni-Ni, and 3NN Ir-Ir pairs are listed in the last two rows

System	Magn.	$\Delta E$	$M(\text{Ni}^{2+}/\text{Ir}^{6+})$
$\text{Sr}_2\text{NiIrO}_6$	FM	0	1.76/1.46
	G-AF	89	1.64/1.28
$\text{Sr}_2\text{Zn}(\text{Ni})\text{IrO}_6$	FM	0	/1.39
	Layered AF	-84	/1.31
$\text{La}_2\text{NiSiO}_6$	FM	0	1.70/
	Layered AF	-19	1.69/
$\text{Sr}_2\text{ZnIrO}_6$	FM	0	/1.42
	Layered AF	-75	/1.34
	Bilayered AF	-42	/1.36
$J_{\text{Ni-Ir}}$	$J'_{\text{Ir-Ir}}$	$J'_{\text{Ni-Ni}}$	$J''_{\text{Ir-Ir}}$
-7.4	9.4, 10.5	2.4	2.2



In contrast, if the Ir-Ir coordination number is reduced as in the low-dimensional iridates, the SOC effect would be manifested. To check this, we also calculate the artificial system  $\text{Sr}_2\text{GaIr}_{0.5}\text{Si}_{0.5}\text{O}_6$  (in  $\text{Sr}_2\text{ZnIrO}_6$  structure) with alternating GaIr and SiGa planes. The  $\text{Ga}^{3+}$ ,  $\text{Ir}^{6+}$  and  $\text{Si}^{4+}$  ions have well comparable ionic sizes, and they make charge balanced and the  $\text{Ir}^{6+}$ - $\text{Ir}^{6+}$  ions only four-coordinated. In this case, the SOC splitting of about 0.5 eV between the  $J = 3/2$  and the  $J = 1/2$  states is well restored as seen in Fig. 5(b), and thus the  $J = 3/2$  and the  $J = 1/2$  states would serve as eigen orbitals in a good approximation<sup>8</sup>.

The above results show that in  $\text{Sr}_2\text{ZnIrO}_6$  and  $\text{Sr}_2\text{NiIrO}_6$ , the delocalized  $\text{Ir}^{6+}$  5d electrons have an insignificant SOC effect due to the band formation in the fcc sublattice. Moreover, the half-filled  $t_{2g}$  subshell of the high-valence  $\text{Ir}^{6+}$  ion has an intrinsic exchange splitting of about 1 eV, see Fig. 3. Both the band effect and the exchange splitting are stronger than the SOC strength, making the SOC ineffective in  $\text{Sr}_2\text{NiIrO}_6$  and  $\text{Sr}_2\text{ZnIrO}_6$ . Our LSDA + U + SOC test calculations indeed show that the  $\text{Ir}^{6+}$  ion has only a small orbital moment of 0.07  $\mu_B$ , being antiparallel to the spin moment of about 1.3  $\mu_B$  reduced from the formal  $S = 3/2$ . Therefore, both  $\text{Sr}_2\text{ZnIrO}_6$  and  $\text{Sr}_2\text{NiIrO}_6$  can be described as an  $\text{Ir}^{6+}$   $S = 3/2$  fcc frustrated system, although  $\text{Sr}_2\text{NiIrO}_6$  itself has an appreciable  $\text{Ni}^{2+}$ - $\text{Ir}^{6+}$  FM coupling.

In summary, using density functional calculations, we find that the newly synthesized isostructural double perovskites  $\text{Sr}_2\text{NiIrO}_6$  and  $\text{Sr}_2\text{ZnIrO}_6$  are insulating and have the formal  $\text{Ir}^{6+}$   $S = 3/2$  fcc sublattice, in addition to the  $\text{Ni}^{2+}$   $S = 1$  sublattice in the former. The delocalized Ir 5d electrons produce long-range magnetic interactions, and the 2NN Ni-Ir AF interaction turns out to be even stronger than the 1NN Ni-Ir FM interaction. Therefore, the leading AF interactions in the fcc Ir sublattice give rise to a magnetic frustration in both  $\text{Sr}_2\text{NiIrO}_6$  and  $\text{Sr}_2\text{ZnIrO}_6$ . As a result, both the cubic compounds appear as a distorted low-temperature antiferromagnet (probably, of type III). Note that the band formation in the high-coordination fcc Ir sublattice and the exchange splitting of the high-valence  $\text{Ir}^{6+}$  ion both make the SOC ineffective, and the long-range interactions of the delocalized 5d electrons (band formation and magnetic coupling) would be taken care of.

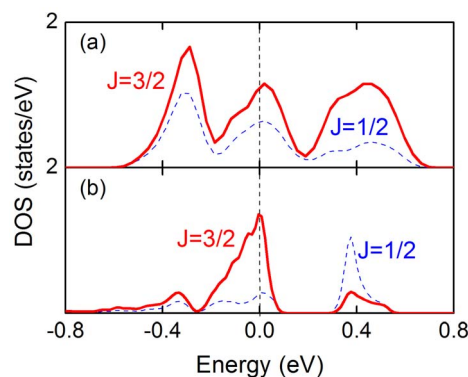


**Figure 5** | The LDA + SOC calculated  $\text{Ir}^{6+}$   $t_{2g}$  DOS projected onto the SOC basis set, the  $J = 3/2$  quartet (solid red curves) and the  $J = 1/2$  doublet (dashed blue curves). (a) In  $\text{Sr}_2\text{ZnIrO}_6$ , the overall mixing of the  $J = 3/2$  and  $J = 1/2$  states is due to the band formation of the delocalized Ir 5d electrons in the fcc Ir sublattice with twelve Ir-Ir coordination. (b) The SOC splitting of about 0.5 eV between the  $J = 3/2$  and the  $J = 1/2$  states is restored upon the reduction of the Ir-Ir coordination to four, which is modeled in the artificial system  $\text{Sr}_2\text{GaIr}_{0.5}\text{Si}_{0.5}\text{O}_6$  (in  $\text{Sr}_2\text{ZnIrO}_6$  structure) with alternating GaIr and SiGa planes.

## Methods

Our calculations were performed using the full-potential augmented plane waves plus local orbital method (WIEN2K code)<sup>27</sup>. We took the structure data of  $\text{Sr}_2\text{NiIrO}_6$  measured by neutron diffraction at RT<sup>17</sup>. The muffin-tin sphere radii are chosen to be 2.8, 2.1, and 1.5 Bohr for Sr, Ni/Ir, and O atoms, respectively. The cutoff energy of 16 Ry is used for plane wave expansion of interstitial wave functions, and  $6 \times 6 \times 4$  k mesh for integration over the Brillouin zone, both of which ensure a sufficient numerical accuracy. SOC is included by the second-variational method with scalar relativistic wave functions. We employ the local spin density approximation plus Hubbard U (LSDA + U) method<sup>28</sup> and use the typical values,  $U = 6$  eV and  $J_H = 0.9$  eV ( $U = 2$  eV and  $J_H = 0.4$  eV), to describe electron correlation of the Ni 3d (Ir 5d) electrons. The calculated Mott insulating state of  $\text{Sr}_2\text{NiIrO}_6$  remains unchanged in a reasonable range of the U values ( $U = 4$ –8 eV for Ni 3d and  $U = 1$ –3 eV for Ir 5d), and the corresponding variation of 1–2 meV for the exchange energy parameters does not affect our discussion and conclusion about the frustrated magnetism.

- Goodenough, J. B. *Magnetism and chemical bond* (Interscience publishers, New York, 1963).
- Kim, B. *et al.* Novel  $J_{\text{eff}} = 1/2$  Mott State Induced by Relativistic Spin-Orbit Coupling in  $\text{Sr}_2\text{IrO}_4$ . *Phys. Rev. Lett.* **101**, 076402 (2008).
- Kim, B. J. *et al.* Phase-sensitive observation of a spin-orbital Mott state in  $\text{Sr}_2\text{IrO}_4$ . *Science* **323**, 1329–1332 (2009).
- Jackeli, G. & Khaliullin, G. Mott Insulators in the Strong Spin-Orbit Coupling Limit: From Heisenberg to a Quantum Compass and Kitaev Models. *Phys. Rev. Lett.* **102**, 017205 (2009).
- Wan, X., Turner, A. M., Vishwanath, A. & Savrasov, S. Y. Topological semimetal and Fermi-arc surface states in the electronic structure of pyrochlore iridates. *Phys. Rev. B* **83**, 205101 (2011).
- Mazin, I. I., Jeschke, H. O., Foyevtsova, K., Valentí, R. & Khomskii, D. I.  $\text{Na}_2\text{IrO}_3$  as a Molecular Orbital Crystal. *Phys. Rev. Lett.* **109**, 197201 (2012).
- Yin, W.-G. *et al.* Ferromagnetic Exchange Anisotropy from Antiferromagnetic Superexchange in the Mixed 3d–5d Transition-Metal Compound  $\text{Sr}_3\text{CuIrO}_6$ . *Phys. Rev. Lett.* **111**, 057202 (2013).
- Ou, X. & Wu, H. Coupled charge-spin-orbital state in Fe- or Co-doped  $\text{Sr}_2\text{IrO}_4$ . *Phys. Rev. B* **89**, 035138 (2014).
- Ou, X. & Wu, H. Impact of spin-orbit coupling on the magnetism of  $\text{Sr}_3\text{MlIrO}_6$  ( $M = \text{Ni}, \text{Co}$ ). *Sci. Rep.* **4**, 4609 (2014).
- Cao, G. *et al.* Novel Magnetism of  $\text{Ir}^{5+}$  ( $5d^4$ ) Ions in the Double Perovskite  $\text{Sr}_2\text{YIrO}_6$ . *Phys. Rev. Lett.* **112**, 056402 (2014).
- Kobayashi, K. I. *et al.* Intergrain tunneling magnetoresistance in polycrystals of the ordered double perovskite  $\text{Sr}_2\text{FeReO}_6$ . *Phys. Rev. B* **59**, 11159 (1999).
- Serrate, D., De Teresa, J. M. & Ibarra, M. R. Double perovskites with ferromagnetism above room temperature. *J. Phys.: Condens. Matter* **19**, 023201 (2007).
- Krockenberger, Y. *et al.*  $\text{Sr}_2\text{CrOsO}_6$ : End point of a spin-polarized metal-insulator transition by 5d band filling. *Phys. Rev. B* **75**, 020404(R) (2007).
- Meetei, O., Erten, O., Randeria, M., Trivedi, N. & Woodward, P. Theory of High Tc Ferrimagnetism in a Multiorbital Mott Insulator. *Phys. Rev. Lett.* **110**, 087203 (2013).
- Paul, A. K. *et al.* Lattice Instability and Competing Spin Structures in the Double Perovskite Insulator  $\text{Sr}_2\text{FeOsO}_6$ . *Phys. Rev. Lett.* **111**, 167205 (2013).
- Morrow, R. *et al.* Independent ordering of two interpenetrating magnetic sublattices in the double perovskite  $\text{Sr}_2\text{CoOsO}_6$ . *J. Am. Chem. Soc.* **135**, 18824–18830 (2013).
- Kayser, P. *et al.* Crystal structure, phase transitions, and magnetic properties of iridium perovskites  $\text{Sr}_2\text{MlIrO}_6$  ( $M = \text{Ni}, \text{Zn}$ ). *Inorg. Chem.* **52**, 11013–11022 (2013).
- Yan, B. *et al.* Lattice-Site-Specific Spin Dynamics in Double Perovskite  $\text{Sr}_2\text{CoOsO}_6$ . *Phys. Rev. Lett.* **112**, 147202 (2014).
- Feng, H. L. *et al.* High-temperature ferrimagnetism driven by lattice distortion in double perovskite  $\text{Ca}_2\text{FeOsO}_6$ . *J. Am. Chem. Soc.* **136**, 3326–3329 (2014).
- Morrow, R., Freeland, J. W. & Woodward, P. M. Probing the Links between Structure and Magnetism in  $\text{Sr}_{2-x}\text{Ca}_x\text{FeOsO}_6$  Double Perovskites. *Inorg. Chem.* **53**, 7983–7992 (2014).
- Wang, H., Zhu, S., Ou, X. & Wu, H. Ferrimagnetism in the double perovskite  $\text{Ca}_2\text{FeOsO}_6$ : A density functional study. *Phys. Rev. B* **90**, 054406 (2014).
- Kanungo, S., Yan, B., Jansen, M. & Felser, C. Ab initio study of low-temperature magnetic properties of double perovskite  $\text{Sr}_2\text{FeOsO}_6$ . *Phys. Rev. B* **89**, 214414 (2014).
- Shender, E. F. & Holdsworth, P. C. W. [Order by Disorder and Topology in Frustrated Magnetic Systems] *Fluctuations and Order: The New Synthesis* [Millonas, M. (ed.)] [259–277] (Springer-Verlag, Berlin, 1996).
- Yamamoto, Y. & Nagamiya, T. Spin Arrangements in Magnetic Compounds of the Rocksalt Crystal Structure. *J. Phys. Soc. Jpn.* **32**, 1248–1261 (1972).
- Henley, C. L. Ordering by disorder: Ground-state selection in fcc vector antiferromagnets. *J. Appl. Phys.* **61**, 3962–3964 (1987).
- Lefmann, K. & Rischel, C. Quantum effects in magnetic structures on the fcc lattice. *Eur. Phys. J. B* **21**, 313–329 (2001).
- Blaha, P., Schwarz, K., Madsen, G., Kvasnicka, D. & Luitz, J. *WIEN2k: An augmented plane wave plus local orbitals program for calculating crystal properties* (Vienna University of Technology, Vienna, 2001).



28. Anisimov, V. I., Solovyev, I. V., Korotin, M. A., Czyzyk, M. T. & Sawatzky, G. A. Density-functional theory and NiO photoemission spectra. *Phys. Rev. B* **48**, 16929–16934 (1993).

### Acknowledgments

This work was supported by the NSF of China (Grant Nos. 11274070 and 11474059), MOE Grant No. 20120071110006, and ShuGuang Program of Shanghai (Grant No. 12SG06). X.O. was also supported by the Outstanding Doctoral Student Project of Fudan University.

### Author contributions

H.W. conceived the idea and designed the research. X.O. performed the calculations, with helps of Z.L., F.F. and H.W. H.W. and X.O. prepared the manuscript.

### Additional information

**Competing financial interests:** The authors declare no competing financial interests.

**How to cite this article:** Ou, X., Li, Z., Fan, F., Wang, H. & Wu, H. Long-range magnetic interaction and frustration in double perovskites  $\text{Sr}_2\text{NiIrO}_6$  and  $\text{Sr}_2\text{ZnIrO}_6$ . *Sci. Rep.* **4**, 7542; DOI:10.1038/srep07542 (2014).



This work is licensed under a Creative Commons Attribution-NonCommercial-NoDerivs 4.0 International License. The images or other third party material in this article are included in the article's Creative Commons license, unless indicated otherwise in the credit line; if the material is not included under the Creative Commons license, users will need to obtain permission from the license holder in order to reproduce the material. To view a copy of this license, visit <http://creativecommons.org/licenses/by-nc-nd/4.0/>